

How to Evaluate Uncertainty Estimates in Machine Learning for Regression?

Laurens Sluijterman

Eric Cator

Department of Mathematics

Radboud University

P.O. Box 9010-59, 6500 GL, Nijmegen, Netherlands

L.SLUIJTERMAN@MATH.RU.NL

E.CATOR@SCIENCE.RU.NL

Tom Heskes

TOM.HESKES@RU.NL

Institute for Computing and Information Sciences

Radboud University

Abstract

As neural networks become more popular, the need for accompanying uncertainty estimates increases. The current testing methodology focusses on how good the predictive uncertainty estimates explain the differences between predictions and observations in a previously unseen test set. Intuitively this is a logical approach. The current setup of benchmark data sets also allows easy comparison between the different methods. We demonstrate, however, through both theoretical arguments and simulations that this way of evaluating the quality of uncertainty estimates has serious flaws. Firstly, it cannot disentangle the aleatoric from the epistemic uncertainty. Secondly, the current methodology considers the uncertainty averaged over all test samples, implicitly averaging out overconfident and underconfident predictions. When checking if the correct fraction of test points falls inside prediction intervals, a good score on average gives no guarantee that the intervals are sensible for individual points. We demonstrate through practical examples that these effects can result in favoring a method, based on the predictive uncertainty, that has undesirable behaviour of the confidence intervals. Finally, we propose a simulation-based testing approach that addresses these problems while still allowing easy comparison between different methods.

Keywords: Neural Networks, Uncertainty, Bootstrap, Dropout, Regression

1. Introduction

Neural networks are, among other things, currently being used in a wide range of regression tasks. These regression tasks cover many different areas. It has become increasingly clear that it is essential to have uncertainty estimates to come with the predictions (Gal, 2016; Pearce, 2020). Uncertainty estimates can be used to make confidence intervals or predictions intervals at a given $100(1 - \alpha)\%$ confidence level. The probability that the true function value falls inside such a confidence interval (CI) should be $100(1 - \alpha)\%$. A $100(1 - \alpha)\%$ prediction interval (PI) is constructed such that the probability that an observation falls inside this interval is $100(1 - \alpha)\%$. The two desirable characteristics of a PI or CI are that they cover the correct fraction of the data while being as small as possible (Khosravi et al., 2011). At the moment a common approach to test a PI is to use a previously unused part of the data and then check which fraction of the observations inside the corresponding PIs.

A noteworthy contribution is the article of Hernández-Lobato and Adams (2015). To compare their proposed method, probabilistic backpropagation, with existing alternatives, they came up with a novel testing procedure. Their testing procedure uses ten publicly available real-world data sets, a fixed number of training epochs, and a fixed number of hidden units and hidden layers. This setup allowed for an effective way of comparing different methods. Many authors subsequently used this setup as a benchmark to compare their uncertainty estimation methods with those of others (Gal and Ghahramani, 2016; Lakshminarayanan et al., 2017; Mancini et al., 2020; Liu and Wang, 2016; Salimbeni and Deisenroth, 2017). It is implicitly assumed that methods that score better also predict the epistemic uncertainty better. This epistemic uncertainty is often used for out-of-distribution detection. The reasoning is that in an area that is previously unseen by the model, the epistemic uncertainty has to be high.

In this article we demonstrate, both theoretically and through simulation experiments, that this testing methodology fails to accurately determine the quality of an uncertainty estimate. Specifically, we show that a good predictive uncertainty on a test set gives no guarantee that the corresponding CIs are correct. Furthermore, covering the correct fraction of points in a test set also does not guarantee that the individual PIs are correct. As a result it is possible to select the wrong method, that may not have sensible PIs or CIs for individual points, as the best. This article consists of six sections, this introduction being the first. Section 2 gives the theoretical framework that is needed to properly discuss uncertainty and explains the current testing methodology. Section 3 gives theoretical drawbacks of the current testing methodology. In Section 4 we propose a simulation-based approach to combat these drawbacks. Section 5 verifies these concerns using simulation results by comparing the current approach to a simulation-based one. Finally, in Section 6 we summarise the conclusions and gives suggestions for future work.

2. Defining the Uncertainty Framework and Testing Methodology

This section consists of two parts. First we go through the terminology necessary to properly discuss uncertainty. In the second part we explain the current testing procedure. For an overview of the various methods to obtain uncertainty estimates, we refer to Khosravi et al. (2011) for early work, and to the review by Hüllermeier and Waegeman (2019) for more recent contributions.

2.1 Defining Uncertainty

Before we can talk about quantifying uncertainty, we need to define precisely what we mean with the term. Throughout this article we consider a regression setting where we have a data set $\mathcal{D} = \{\mathbf{x}_n, y_n\}_{n=1}^N$ consisting of N i.i.d. datapoints with $\mathbf{x} \in \mathbb{R}^d$ and $y \in \mathbb{R}$. We assume that our observations are a combination of an unknown function and a noise term:

$$y_i = f(\mathbf{x}_i) + \epsilon_i.$$

If the distribution of ϵ_i given \mathbf{x}_i does not depend on \mathbf{x}_i , then we have *homoscedastic* noise. If the distribution of ϵ_i given \mathbf{x}_i depends on \mathbf{x}_i , we have *heteroscedastic* noise. The uncertainty due to ϵ_i is often referred to as the *aleatoric uncertainty, irreducible variance, or data*

noise variance.

In a regression setting we aim to produce an estimate $\hat{f}(\mathbf{x})$ of $f(\mathbf{x})$. There is an error between the estimate and the true function:

$$\epsilon_{\omega,i} = \hat{f}(\mathbf{x}_i) - f(\mathbf{x}_i).$$

The uncertainty due to $\epsilon_{\omega,i}$ is typically called the *model uncertainty*, *approximation uncertainty* or *epistemic uncertainty*. In this paper we use following terminology. Epistemic uncertainty is the total uncertainty that we can in theory get rid of by having more data and better models. Epistemic uncertainty can be further dissected in two parts: the approximation uncertainty that takes into account that we do not have the optimal model within our class of models, and model uncertainty that takes into account that the true function may not even be in our hypothesis class. This dissection is illustrated in Figure 1.

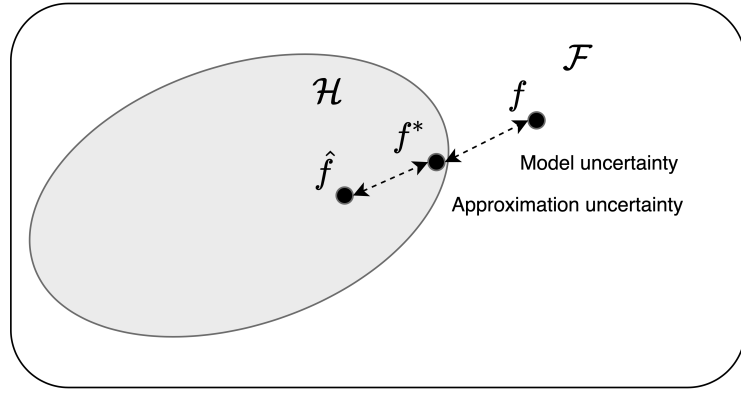


Figure 1: This figure illustrates the different components that make up the epistemic uncertainty. All possible functions that our neural network can make are denoted with \mathcal{H} . This \mathcal{H} is contained in \mathcal{F} , all possible functions that map \mathbf{x} to y . On the one hand we do not know if the true function f is inside our hypothesis class. This causes the model uncertainty. On the other hand we do not know if the \hat{f} that we arrived at after training is even the best function in our hypothesis class, f^* . This causes the approximation uncertainty.

The argument is often made that neural networks are able to approximate nearly any function arbitrarily well (Hornik et al., 1989; Lu et al., 2017). This means that the true function, $f(\mathbf{x})$, should be in our hypothesis class. We therefore assume that the epistemic uncertainty is mainly determined by the uncertainty in the parameters of the network.

To summarize, we are dealing with different types of uncertainty: aleatoric uncertainty that is caused by the inherent randomness of the observations, and epistemic uncertainty that we could in theory get rid of by collecting more data. These two sources of uncertainty can be added to obtain the predictive uncertainty,

$$\epsilon_{predictive,i} = \epsilon_i + \epsilon_{\omega,i}.$$

The predictive uncertainty describes the difference between the predicted value and the observation:

$$\epsilon_{predictive,i} = y_i - \hat{f}(\mathbf{x}_i).$$

2.2 The Current Testing Methodology

The currently popular procedures for testing uncertainty estimates in neural networks are largely influenced by Hernández-Lobato and Adams (2015). In this article the authors systematically test their uncertainty estimates on ten different real-world data sets. The data sets that are being used are listed in Table 1.

data set	N	d	Description
<i>Boston Housing</i>	506	13	Housing prices in suburbs of Boston as a function of covariates such as crime rates and mean number of rooms
<i>Concrete Compression Strength</i>	1030	8	Concrete compressive strength as a function of covariates such as temperature and age
<i>Energy Efficiency</i>	768	8	The energy efficiencies of buildings as a function of covariates such as wall area, roof area, and height
<i>Kin8nm</i>	8192	8	The forward kinematics of an 8 link robot arm
<i>Naval propulsion</i>	11,934	16	A simulated data set giving the propulsion behaviour of a naval vessel
<i>Combined Cycle Power Plant</i>	9568	4	The net hourly electrical energy output as a function of temperature, ambient pressure, relative humidity, and exhaust vacuum
<i>Protein Structure</i>	45,730	9	Physicochemical properties of protein tertiary structure
<i>Wine Quality Red</i>	1599	11	Wine quality as a function of physicochemical tests such as density, pH, and sulphate levels
<i>Yacht Hydrodynamics</i>	308	6	Air resistance of sailing yachts as a function of covariates such as length-beam ratio, prismatic coefficient, or beam-draught ratio
<i>Year Prediction MSD</i>	515,345	90	The release year of a song based on audio features

Table 1: The ten different regression data sets that are currently being used as a benchmark for estimating the quality of uncertainty estimates. The number of instances, N , number of covariates, d , and a short description are given.

Using these data sets, they carry out the following procedure.

Step 1: Standardize the data so that it has zero mean and unit variance.

Step 2: Split the data in a training and test set. They apply a 90/10 split.

Step 3: Train the network using 40 epochs and update the weights of the network after each data point. They use a network with one hidden layer containing 50 hidden units. For the two largest data sets, *Protein Structure* and *Year Prediction MSD*, they chose 100 hidden units.

Step 4: Repeat steps 2 and 3 a total of 20 times and report the average root mean squared error (*RMSE*) and loglikelihood (*LL*) on the test set and their standard deviations. They undo the standardization before calculating the *RMSE* and *LL*.

This setup has subsequently been used in multiple articles (Gal and Ghahramani, 2016; Lakshminarayanan et al., 2017; Mancini et al., 2020; Liu and Wang, 2016; Salimbeni and Deisenroth, 2017). The loglikelihood measures how well the distribution of y given \mathbf{x} is approximated. This measures both how well the function, $f(\mathbf{x})$, and how well the predictive variance are estimated. The loglikelihood therefore does not directly tell us if the uncertainty estimates are better or worse. It is possible to use other measures. Pearce et al. (2018), for instance, use the same data sets but the metric PICP, which we explain now. In practice one would ideally want a prediction interval at a given confidence level that gives a probability that the true value falls inside that interval. These intervals are tested on the test set by calculating the so-called Prediction Interval Coverage Probability, or PICP. This is the fraction of observations in the test set that fall inside the corresponding PIs:

$$\text{PICP} := \frac{1}{n_{test}} \sum_{i=1}^{n_{test}} \mathbb{1}_{y_i \in [L(\mathbf{x}_i), R(\mathbf{x}_i)]}, \quad (1)$$

where n_{test} is the size of the test set, y_i is the observation of datapoint i , and $L(\mathbf{x}_i)$ and $R(\mathbf{x}_i)$ are the lower and upper bound of the PI of y_i . Analogously we can define the CICP for a CI:

$$\text{CICP} := \frac{1}{n_{test}} \sum_{i=1}^{n_{test}} \mathbb{1}_{f(\mathbf{x}_i) \in [LC(\mathbf{x}_i), RC(\mathbf{x}_i)]},$$

where $LC(\mathbf{x}_i)$ and $RC(\mathbf{x}_i)$ are the lower and upper bound of the CI of $f(\mathbf{x}_i)$. It is, however, impossible to calculate the CICP for these data sets as we do not know the true function $f(\mathbf{x})$. The average width of the intervals is also reported since we prefer intervals that capture the correct fraction of the data while being as narrow as possible.

3. Theoretical Shortcomings of the Current Testing Methodology

In this section we discuss four problems with the aforementioned method of testing the quality of uncertainty estimates on a single test set. We first identify two problems that arise when using either the PICP or loglikelihood. The first problem is that it is impossible to determine whether the quality of the estimate is determined by the estimate of the aleatoric or by the estimate of the epistemic uncertainty. Secondly, the epistemic uncertainty estimates are generally not independent for different values of \mathbf{x} . This means that the quality of these estimates cannot in general be determined by averaging over multiple test samples. Furthermore, we identify two additional problems, one for the PICP and one for the loglikelihood. When using the PICP, a good score can be achieved by only being

correct on average. With the loglikelihood, a better score can be achieved by having a better estimate of the true function, even with a worse estimate of the uncertainty.

3.1 Which Uncertainty Estimate is Correct?

Suppose we have an estimate for the aleatoric uncertainty, ϵ_i , and the epistemic uncertainty, $\epsilon_{\omega,i}$. These two estimates can be combined to obtain a predictive uncertainty estimate. Suppose we compare two methods, A and B , by carrying out the test as described in the previous section. We can compare the methods by looking at the PICP or loglikelihood. If method A gets a better score than method B , it is unclear why. It is possible that the estimate for the epistemic uncertainty in method A was much worse than for method B but that this was compensated by a superior estimate of the aleatoric uncertainty. Yet another possibility is that both estimates are incorrect but result, more or less, in the correct total uncertainty. For the practitioner, interested in the performance on a single problem and a single data set, this may not be an issue. When testing if a novel method works well, however, it is. Getting the epistemic uncertainty correct is also important when you are more interested in the true function than in the observations. We can for example think of a physicist that measures a process and is dealing with noisy measurements. Getting the epistemic uncertainty correct is also crucial for out-of-distribution detection. In areas where there is a limited amount of data we expect our network to be more uncertain and we would like to quantify this with the epistemic uncertainty. Currently, these uncertainty estimation methods are also being used for out-of-distribution detection. It is therefore crucial to know if the epistemic uncertainty estimate is correct or not.

3.2 The Epistemic Uncertainty is not Independent

The epistemic uncertainty estimates that we obtain are generally not independent for different values of \mathbf{x} . This poses a serious problem in evaluating the quality of the uncertainty estimates. The uncertainty in the output of the network is a result of the uncertainties in the weights of the network. These uncertainties are the same for different values of \mathbf{x} . This is not to say that the epistemic uncertainties in the outcome of a network for different values of \mathbf{x} are equal. Different values of \mathbf{x} interact more heavily with different parts of the network after all. The fallacy of treating these uncertainty estimates as independent can be best illustrated through a simple example.

We consider a linear model without a bias term,

$$y_i = ax_i + \epsilon_i.$$

The epistemic uncertainty considers the uncertainty in our estimate \hat{a} . For this example we assume that the true function is of the form $f(x) = ax$, meaning that the true function is within our hypothesis class. Suppose we have a perfectly calibrated procedure to construct a 95% CI for a . This means that an interval constructed by that procedure will contain the true value of a 95% of the time. We can translate the CI of a to a CI of $f(x_i) = ax_i$. Since the true a is either inside our CI or not, $f(x_i)$ is for all x_i either inside the CI or not. This results in a CICP of either 0 or 1, even though the uncertainty estimate is perfectly calibrated. This illustrates that we cannot test the quality of our CI by simply looking at

the fraction of points in a test set that are in our interval. This example is illustrated in Figure 2.

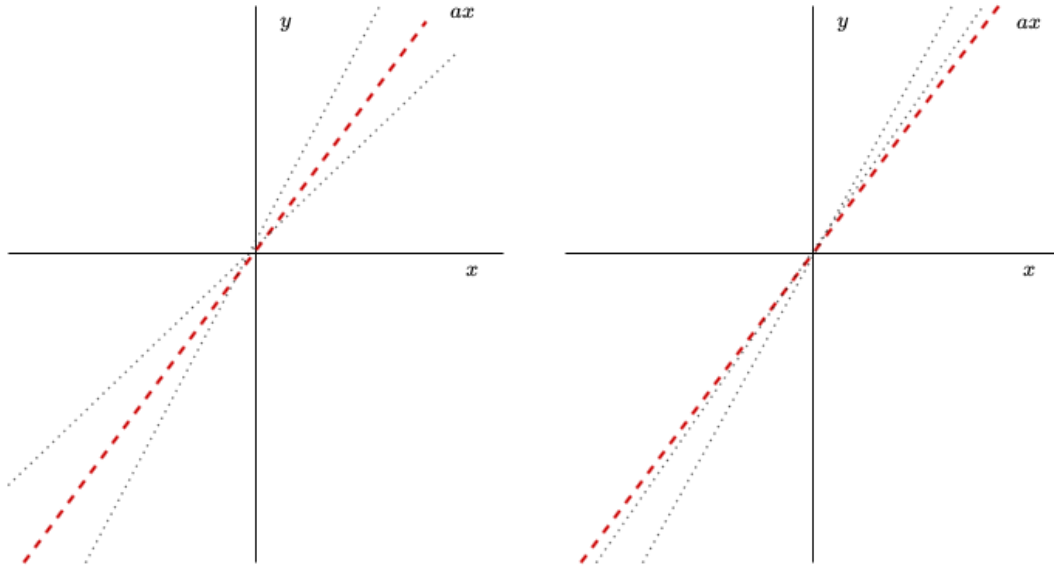


Figure 2: The dashed red line gives the true function $f(x) = ax$. The two dotted black lines give the confidence interval. In the left figure the true function falls inside our confidence interval, in the right figure it does not. It is clear that the measure CICP will either give 1 or 0, even when we have a method that gives a perfect 95% confidence interval. This illustrates that the epistemic uncertainty estimates are not independent.

We note that the loglikelihood is also affected by this problem. Even if we determine the epistemic uncertainty perfectly, such that $f(x)$ falls within one standard deviation with the correct probability, the loglikelihood is still highly dependent on whether or not the true function is close to the prediction. Since all the $f(x)$ are dependent, we cannot determine the quality of the epistemic uncertainty by looking at the loglikelihood of $f(x)$ given $\hat{f}(x)$ and $\hat{\sigma}_\omega(x)$ in a single dataset.

In practice it is not possible to calculate the CICP or the loglikelihood of the function values as the true function values are not available for real world data sets. The quality of the CI is therefore indirectly measured through the PICP or the loglikelihood of the observations. PICP scores close to the chosen confidence levels are reported in the literature (Khosravi et al., 2011). If the epistemic uncertainty is not independent, we would not expect this. We can explain this as follows. First of all, the example of a linear model is the most dependent case imaginable. In general the dependence will be weaker. Secondly, it is possible that the epistemic uncertainty is much smaller than the aleatoric uncertainty. In this case you also expect to get a PICP score close to the chosen confidence level if the aleatoric uncertainty is estimated correctly. It would therefore seem that a good PICP score

is at least a guarantee that the aleatoric uncertainty estimate is correct. We demonstrate in the following subsection that even this is not the case.

3.3 Being Correct on Average Gives a Good PICP Score

It is possible to get a good PICP score while only estimating the aleatoric uncertainty correctly *on average*. We illustrate this in Figure 3. Assume that the true function is the constant zero function, $f(x) = 0$, and that our estimate of the function is very good, $\hat{f}(x) \approx 0$. The dashed blue lines give plus and minus one time the true standard deviation of the data. Suppose that we use a homoscedastic estimate of this standard deviation, the dotted black line, and that this estimate has on average the correct size. The PICP score of the 68% PI made with our homoscedastic estimate is 0.65 in this example. The intervals are too wide for some x and too small for others but *on average* we capture the correct fraction of the data. We are not able to see that our estimate is wrong by simply evaluating the PICP on a test set.

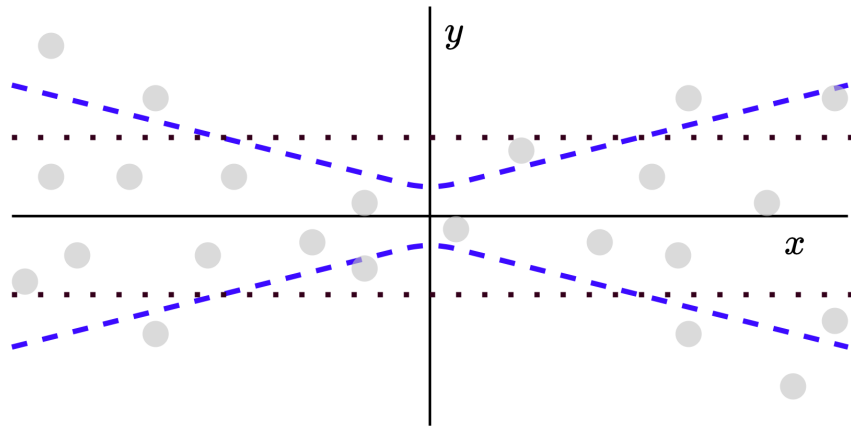


Figure 3: This figure illustrates that estimating the aleatoric uncertainty correctly can result in a PICP close to the chosen confidence level. We assume that the epistemic uncertainty is comparably very small. The true function, $f(x)$, is the constant zero function. The dashed blue line gives $\pm 1\sigma(x)$. The dotted black line gives $\pm 1\hat{\sigma}(x)$. On average the aleatoric uncertainty estimate is correct and its corresponding PI captures the correct fraction of the data in this case. In this example, we do not notice that our uncertainty estimate is wrong.

We also want to stress that with a one-dimensional output it is often possible to get close to the desired PICP value on an unseen part of the training set by tuning the hyperparameters. Monte Carlo dropout for instance has the aleatoric variance as a hyperparameter. If the PICP value is too low, it is possible to tune this parameter until it is correct. If the test set resembles the training set, it is unsurprising that a good PICP score can also be achieved on this set. In Section 5 we elaborate on this.

3.4 Loglikelihood Also Measures Accuracy

The loglikelihood of y given $\hat{f}(x)$ and $\hat{\sigma}(x)$ measures both the quality of $\hat{f}(x)$ and $\hat{\sigma}(x)$. It is therefore possible to get a higher loglikelihood even if the uncertainty estimate is actually worse. This problem was identified in a classification setting by Ashukha et al. (2020). A practical example can be found in the paper on Monte Carlo dropout (Gal and Ghahramani, 2016). The authors compare their method to a, at that time, popular variational inference method (Graves, 2011) and probabilistic backpropagation (Hernández-Lobato and Adams, 2015). They are able to get superior or comparable loglikelihood scores on the test sets of all ten datasets in Table 1. However, they also get lower RMSE on the test sets for nine of the ten datasets. It is not immediately clear if the better loglikelihood is the result of a better estimate of $f(x)$ or of $\sigma(x)$.

For the rest of this paper we focus on the PICP for the following two reasons. Firstly, it aims to measure purely the quality of the uncertainty estimate. Secondly, it is clearer what the PICP *should* be, namely $1 - \alpha$. It is therefore more illustrative to demonstrate the shortcomings mentioned in this section using this metric. In Section 5 we demonstrate that a good PICP score gives no guarantees on the quality of the estimates of either the aleatoric or the epistemic uncertainty. We additionally demonstrate that the aforementioned problems can be overcome by using a simulation-based testing approach, which we describe in the following section.

4. Simulation-Based Testing

In this section we propose a simulation-based framework for testing uncertainty estimates. There are two main advantages to using simulated data:

1. The true function, $f(\mathbf{x})$, and the true variance of the noise, $\sigma^2(\mathbf{x})$, are known. This makes it possible to directly test the quality of the epistemic and aleatoric uncertainty estimates. Without the true function and noise variance it is only possible to test the predictive uncertainty.
2. It is possible to test the coverage probabilities of CIs and PIs per \mathbf{x} .

We propose to look at the average coverage, per \mathbf{x} , over a large number of simulations. To avoid confusion we refer to this as the coverage fraction instead of the coverage probability, to distinguish averaging over the test set and averaging over different simulations. Specifically, we define the PICF and CICF as follows:

$$\text{PICF}(\mathbf{x}) := \frac{1}{n_{\text{simulations}}} \sum_{j=1}^{n_{\text{simulations}}} \mathbb{P}(Y \in [L^{(j)}(\mathbf{x}), R^{(j)}(\mathbf{x})] \mid \mathbf{x}), \quad (2)$$

where Y is the random variable of which the realisations are the observations, and $L^{(j)}(\mathbf{x}), R^{(j)}(\mathbf{x})$ are the lower and upper bound respectively of the PI of Y in simulation j . Since we simulate the data, we know the true function and variance of the noise. If we use normally distributed noise for example, we can calculate the probability that the observation y belonging to \mathbf{x}

falls inside the PI as

$$\mathbb{P}\left(Y \in [L^{(j)}(\mathbf{x}), R^{(j)}(\mathbf{x})] \mid \mathbf{x}\right) = \Phi\left(\frac{R^{(j)}(\mathbf{x}) - f(\mathbf{x})}{\sigma(\mathbf{x})}\right) - \Phi\left(\frac{L^{(j)}(\mathbf{x}) - f(\mathbf{x})}{\sigma(\mathbf{x})}\right),$$

where Φ is the CDF of a standard normal Gaussian. It is also possible to actually simulate y and check if it falls inside the PI or not. This gives less consistent results, however, making comparison between methods less precise.

Analogously we define the Confidence Interval Coverage Fraction:

$$\text{CICF}(\mathbf{x}) := \frac{1}{n_{\text{simulations}}} \sum_{j=1}^{n_{\text{simulations}}} \mathbb{1}_{f(\mathbf{x}) \in [LC^{(j)}(\mathbf{x}), RC^{(j)}(\mathbf{x})]},$$

where $f(\mathbf{x})$ is the true function value, and $LC^{(j)}(\mathbf{x}), RC^{(j)}(\mathbf{x})$ are the lower and upper limit of the CI of $f(\mathbf{x})$ in simulation j . Note that if we have n_{test} observations in our test set, then we obtain n_{test} different computations of $\text{PICF}(\mathbf{x})$ and $\text{CICF}(\mathbf{x})$. These evaluations can be plotted in a histogram to see if the coverage fractions match the chosen confidence levels. In a one-dimensional setting we can also plot the PICF and CICF as a function of x .

If we construct a $100(1 - \alpha)\%$ PI or CI, then we would ideally want the $\text{PICF}(\mathbf{x})$ and the $\text{CICF}(\mathbf{x})$ to be $1 - \alpha$ for every \mathbf{x} . As a quantitative measure for the quality of the PI and CI we propose to use the Brier score, where lower is better. For the PICF this yields

$$\text{BS} = \frac{1}{n_{\text{test}}} \sum_{i=1}^{n_{\text{test}}} (\text{PICF}(\mathbf{x}_i) - (1 - \alpha))^2. \quad (3)$$

A Brier score for the PICF for instance is lower if the average is close to the desired value of $(1 - \alpha)$ while having a low variance. We observe this by looking at the bias-variance decomposition

$$\mathbb{E}\left[(\text{PICF}(\mathbf{x}) - (1 - \alpha))^2\right] = \mathbb{E}[\text{PICF}(\mathbf{x}) - (1 - \alpha)]^2 + \mathbb{V}[\text{PICF}(\mathbf{x})].$$

The PICP only measures the bias. This means that simply being correct on average instead of for all \mathbf{x} results in a worse score when using the PICF . We can use the same measure to quantify the quality of a CI. The suggested simulation-based approach can be summarized as follows.

Step 1: Standardize the data such that it has zero mean and unit variance.

Step 2: Split the covariates (X) in a training and test set ($X_{\text{train}}, X_{\text{test}}$), using the same split when comparing different uncertainty estimation methods.

Step 3: Simulate Y_{train} and Y_{test} , use the uncertainty estimation method to obtain the PIs and CIs at different confidence levels, for instance 95, 90, 80, and 70%. Repeat this 100 times.

Step 4: Calculate the PICF and CICF for each \mathbf{x} .

Step 5: Evaluate the relevant metrics, for instance the Brier score and the average width.

To simulate data, we propose two possibilities. The first option is to take a known test function and a noise term. The advantage of this is having total control over the setup. The disadvantage is that it may not be representative of real-world situations. A second option is to use simulations that are based on real-world data sets. The current benchmark data sets are good candidates. In the last part of the next section we demonstrate a simulation setup for the popular Boston Housing data set.

5. Experimental Demonstration of the Advantages of Simulation-based Testing

In this section we experimentally demonstrate the theoretical shortcomings raised in Section 3 and show how these issues can be resolved by using a simulation-based approach. As an illustration, we use two methods that are easy to implement: the naïve bootstrap (Heskes, 1997), and Monte Carlo dropout (Gal and Ghahramani, 2016). With these two approaches, we first show that a good PICP does not imply that the individual aleatoric and epistemic uncertainty estimates are correct. Since we know the true underlying function we can look at the CICP directly and verify its correctness. We proposed in the previous section to average over simulations per \mathbf{x} , instead of averaging over \mathbf{x} in a single test set. We demonstrate that this is useful by observing that having the desired CICP gives no guarantees that the CIs are correct for an individual \mathbf{x} . Most importantly we demonstrate that it is possible to favor the wrong method when using the predictive performance on a test set as the measure. We end this section by setting up a simulation based on the Boston Housing data set.

5.1 Monte Carlo Dropout and the Naive Bootstrap

The uncertainty estimation methods used in this section assume that both the aleatoric and epistemic uncertainty are normally distributed:

$$\epsilon_i \sim \mathcal{N}(0, \sigma^2(\mathbf{x}_i)), \quad \text{and} \quad \epsilon_{\omega,i} \sim \mathcal{N}(0, \sigma_{\omega}^2(\mathbf{x}_i)).$$

These two uncertainties can be combined to jointly make up the total predictive uncertainty. The methods additionally assume that both uncertainty estimates are independent. This independence allows us to add up both the variances to obtain the variance of the predictive uncertainty.

We use the bootstrap setup from Heskes (1997). This setup outputs a CI as described in Algorithm 1.

Algorithm 1: Pseudocode to obtain a CI for $f(\mathbf{x})$ using an implementation of the naïve bootstrap approach as described by Heskes (1997).

```

1 for  $i$  in  $1:M$  do
2   Resample  $(X, Y)$  pairwise with replacement, denote this sample with
    $(X^{(i)}, Y^{(i)})$ ;
3   Train an ANN on  $(X^{(i)}, Y^{(i)})$  that outputs  $\hat{f}_i(\mathbf{x})$ ;
4   Define  $\hat{f}(\mathbf{x}) = \frac{1}{M} \sum_{i=1}^M \hat{f}_i(\mathbf{x})$ ;
5   Calculate  $\hat{\sigma}_{\omega}^2(\mathbf{x}) = \frac{1}{M-1} \sum_{i=1}^M \left( \hat{f}_i(\mathbf{x}) - \hat{f}(\mathbf{x}) \right)^2$ ;
6   CI =  $[\hat{f}(\mathbf{x}) - t_{1-\alpha/2}^M \hat{\sigma}_{\omega}(\mathbf{x}), \hat{f}(\mathbf{x}) + t_{1-\alpha/2}^M \hat{\sigma}_{\omega}(\mathbf{x})]$ ;
7 return: CI;

```

In this algorithm $t_{1-\alpha/2}^M$ is the $1 - \frac{\alpha}{2}$ quantile of a t -distribution with M degrees of freedom. We train networks with 40, 30, and 20 neurons respectively and *ReLU* activation functions for 40 epochs. In order to arrive at a prediction interval we also need an estimate

of the aleatoric uncertainty. Assuming homoscedastic noise, we take

$$\hat{\sigma}^2 = \frac{1}{n_{val}} \sum_{j=1}^{n_{val}} \max \left(\left(y_j - \hat{f}(\mathbf{x}_j) \right)^2 - \frac{1}{M-1} \sum_{i=1}^M \left(\hat{f}_i(\mathbf{x}_j) - \hat{f}(\mathbf{x}_j) \right)^2, 0 \right). \quad (4)$$

Note that we use a small additional validation set to determine $\hat{\sigma}$. With both $\hat{\sigma}$ and $\hat{\sigma}_\omega(\mathbf{x})$ we construct the prediction interval

$$\text{PI} = \left[\hat{f}(\mathbf{x}) - t_{1-\alpha/2}^M \sqrt{\hat{\sigma}_\omega^2(\mathbf{x}) + \hat{\sigma}^2}, \quad \hat{f}(\mathbf{x}) + t_{1-\alpha/2}^M \sqrt{\hat{\sigma}_\omega^2(\mathbf{x}) + \hat{\sigma}^2} \right].$$

A different approach to obtain uncertainty estimates is Monte Carlo dropout (Gal and Ghahramani, 2016). The easy implementation makes this method very popular. We first train a network with dropout enabled and then keep dropout enabled while making predictions. The article shows that, under certain conditions, this is equivalent to sampling from an approximate posterior. The standard deviation of these forward passes is used as an estimate of the epistemic uncertainty. The inverse of the hyperparameter τ gives the estimate of the variance of the aleatoric uncertainty. Algorithm 2 describes the procedure in more detail.

Algorithm 2: Pseudocode to obtain a confidence and prediction interval using Monte Carlo dropout.

- 1 Train an ANN with dropout enabled on (X, Y) ;
- 2 Define $\hat{f}(\mathbf{x}) = \frac{1}{B} \sum_{i=1}^B \hat{f}_i(\mathbf{x})$, where $\hat{f}_i(\mathbf{x})$ is a forward pass through to network. For each i different weights are dropped;
- 3 Define $\hat{\sigma}_\omega^2(\mathbf{x}) := \frac{1}{B-1} \sum_{i=1}^B \left(\hat{f}(\mathbf{x}) - \hat{f}_i(\mathbf{x}) \right)^2$;
- 4 CI = $[\hat{f}(\mathbf{x}) - z_{1-\alpha/2} \hat{\sigma}_\omega(\mathbf{x}), \hat{f}(\mathbf{x}) + z_{1-\alpha/2} \hat{\sigma}_\omega(\mathbf{x})]$;
- 5 PI = $[\hat{f}(\mathbf{x}) - z_{1-\alpha/2} \sqrt{\hat{\sigma}_\omega^2(\mathbf{x}) + \tau^{-1}}, \hat{f}(\mathbf{x}) + z_{1-\alpha/2} \sqrt{\hat{\sigma}_\omega^2(\mathbf{x}) + \tau^{-1}}]$;
- 6 **return:** CI, PI;

The two hyperparameters τ and p (the dropout rate) are very important for the uncertainty estimate. The uncertainty estimates can be made small by picking τ large, resulting in a low aleatoric uncertainty estimate, and p small, resulting in little variance in the forward passes and thus a small epistemic uncertainty estimate. We use a manual grid search over τ and p that optimises the PICP at a 68% confidence level. We use 80% of the training data and evaluate the PICP on the remaining 20%. During the experiments we use the entire training set. It is important to note that with a one-dimensional output we can get close to almost any PICP score on the training data by tuning these two hyperparameters.

5.2 A Toy Example with Homoscedastic Noise

In this subsection we demonstrate that a good on average performance on a single test set gives no guarantees for the actual quality of the uncertainty estimate. We simulated data from $y = f(x) + \epsilon$ with $f(x) = (2x - 1)^3$, and $\epsilon \sim \mathcal{N}(0, (0.2)^2)$. The training and test set both contain 1000 data points. The bootstrap method has an additional 150 validation data points to determine the aleatoric noise. The x values are drawn uniformly from the interval $[-0.5, 0.5]$. A total of $M = 50$ bootstrap networks are trained in order to construct a CI and

PI for each x in the test set using the bootstrap approach. For the dropout approach we used $B = 100$ forward passes through the network. We repeated these procedures for estimating prediction and confidence intervals for 100 simulations of randomly drawn training and test sets.

In Figure 4 we see that both methods give a PICP that is very close to the desired values of 0.9 and 0.8 in each of the 100 simulations. Note that when simply using one data set we would only have 1 PICP value.

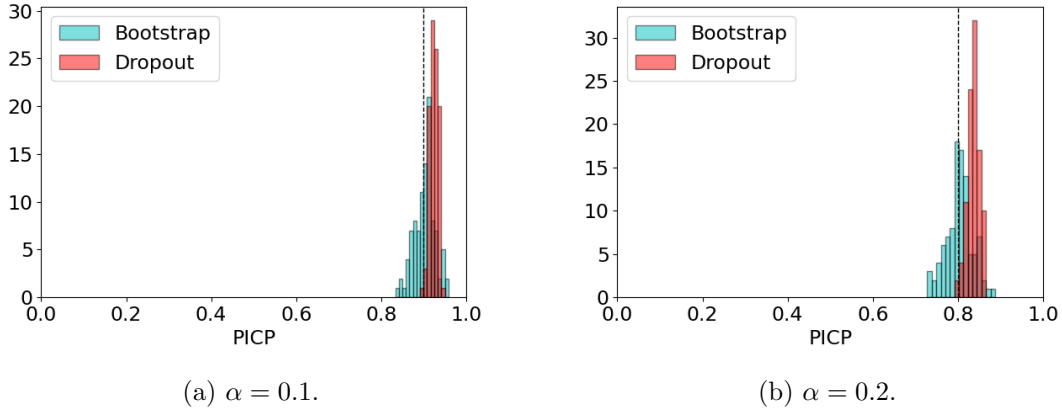


Figure 4: These histograms give 100 evaluations of the PICP, at a $(1 - \alpha)$ confidence level using both the bootstrap and dropout approach. The PICP captures the fraction of data points in the test set for which the observations y falls inside the corresponding prediction interval. The data is simulated from $y = f(x) + \epsilon$ with $f(x) = (2x - 1)^3$, and $\epsilon \sim \mathcal{N}(0, (0.2)^2)$. The details of the construction of the PIs can be found in Section 5.1. From these histograms we can see that in a single simulation we would have a good performance of the PI on the test set with either method.

As we argued in Section 3.1, however, it is not clear that a good PICP indicates that the CIs are good. In a real-world scenario we would not have access to the true function, $f(x)$, and we would not be able to calculate the CICP. In this case, however, we are. In Figure 5 we can see that the CICP values were not that great for most simulations. Especially note the behaviour of the dropout method in the left figure. We also see that there is a lot of variance between the CICP values of individual simulations. This could be caused by the dependence of the epistemic uncertainty estimates that we noted in Section 3.2. However, even *if* these CICP values would have been perfect, it is still possible that this happens because the CIs are only correct on average. CIs that are much too large for some x can be countered by CIs that are much too small for other x .

This effect can be seen when we actually look at the coverage fraction per value of x calculated over all the simulations, the CICF, as we proposed in the previous section. To reiterate, for the PICP and CICP we average over test data points and then provide a histogram over simulations, whereas for the PICF and CICF values we average over

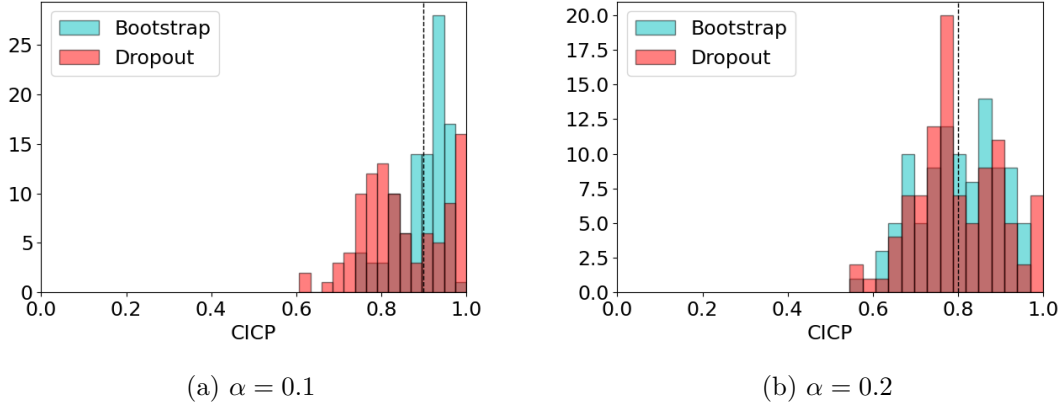


Figure 5: These histograms give 100 evaluations of CICP, at a $(1 - \alpha)$ confidence level. Each point in the histograms gives the fraction of datapoints in the test set of a new simulation for which the true function value $f(x)$ falls inside the corresponding confidence interval. Each simulation has its own CICP value. The same setup was used as in Figure 4. We observe that the good PICP values from Figure 4 do not translate to good CICP values.

simulations. In Figure 6(b) we can see that for some values of x the CIs contained the true value $f(x)$ in every simulation while hardly ever for other values of x . In Figure 6(a) we see that in this set of simulations the PIs are the pretty accurate for most values of x and not only on average.

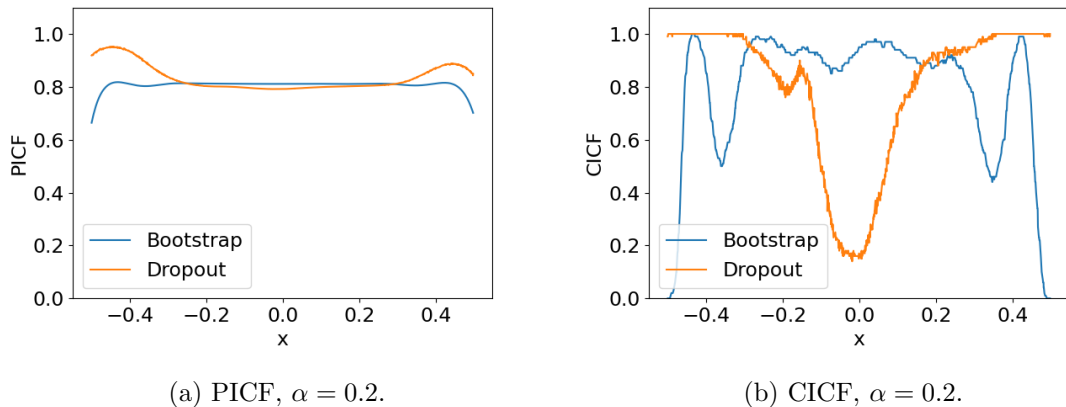


Figure 6: The PICF and CICF plotted as a function of x . The PIs appear to be correct for most x while the CIs are too large or too small most of the time. The PIs and CIs were constructed at an 80% confidence level.

5.3 A Toy Example with Heteroscedastic Noise

In the previous example, the PIs behaved well. It is, however, also possible for the PICP to be good only because the PIs are correct on average. Figure 7 illustrates this point. We repeat the simulation but now using a noise term with a standard deviation of $0.1 + x^2$. Both the bootstrap and dropout method assume a homoscedastic noise. Figure 7 illustrates that the PICP does not show us that the aleatoric uncertainty estimate is wrong. Even worse, it can point in the wrong direction. We can favor the worse method if we would use the coverage fraction on a test set as our metric. Note that in Figure 7(a) we can see that in most simulations the bootstrap approach had a comparable PICP score compared to the dropout method. On average, the PICP score of the bootstrap method was even slightly better (0.86 versus 0.83). Figure 7(b), however, shows that this is only the case because for some values of x the coverage fraction was too high and for others too low, resulting in a good performance on average. According to the Brier score, dropout performed better in this specific case: it has much lower variance, which more than compensates for the higher bias.

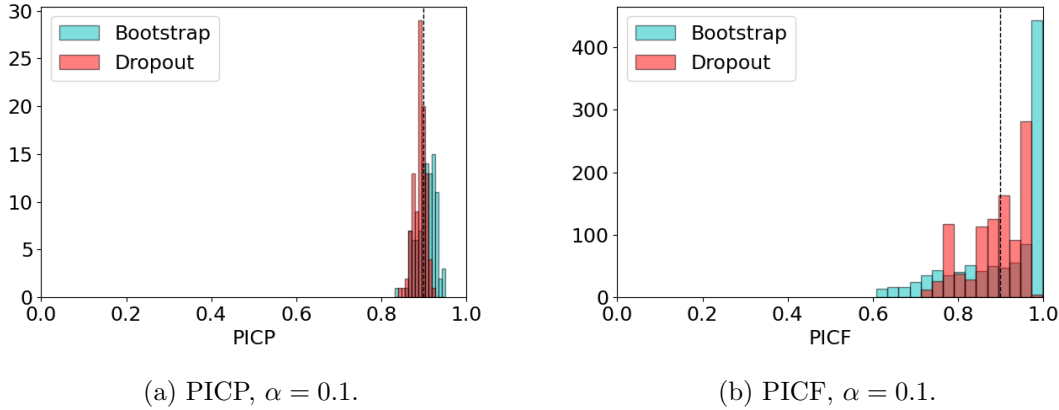


Figure 7: These histograms give the different PICP and PICF values using the bootstrap and dropout approach. The PICP is obtained by calculating the coverage fraction of the PIs on the test set in each simulations. The PICF is obtained by calculating the coverage fraction of the PIs taken over all the simulations. In this simulation we constructed 90% PIs. Bootstrap has a Brier score of 0.011, dropout has a Brier score of 0.005. We see that a good PICP score does not imply that the PIs are sensible for individual values of x .

5.4 Out-of-Distribution Detection

A desirable property of a confidence interval is that it gets larger in areas where there is a limited amount of data. It is not evident that a good performance on a test set guarantees this effect. In Figure 8 we use the same function as in our example with homoscedastic noise, but simulate our x values from a bimodal distribution instead of uniformly. Both models are trained using 250 data points and evaluated on a test set of size 1000. When

making 80% CIs and PIs, the bootstrap and dropout methods give a PICP score of 0.868 and 0.831 respectively. The PICP score of the dropout method is closer to desired value of 0.8 and one might conclude from this that this method is better able to construct CIs. If we actually look at the CIs, however, we see that the behaviour is not as desired and that the bootstrap approach created more sensible CIs. The CIs of the bootstrap method get larger in the area around 0 where there is a limited amount of data and smaller around -0.4 and 0.3 where there is more data. The intervals created by using Monte Carlo dropout do the exact opposite, even though the performance on a single test set was better when using the PICP as a metric.

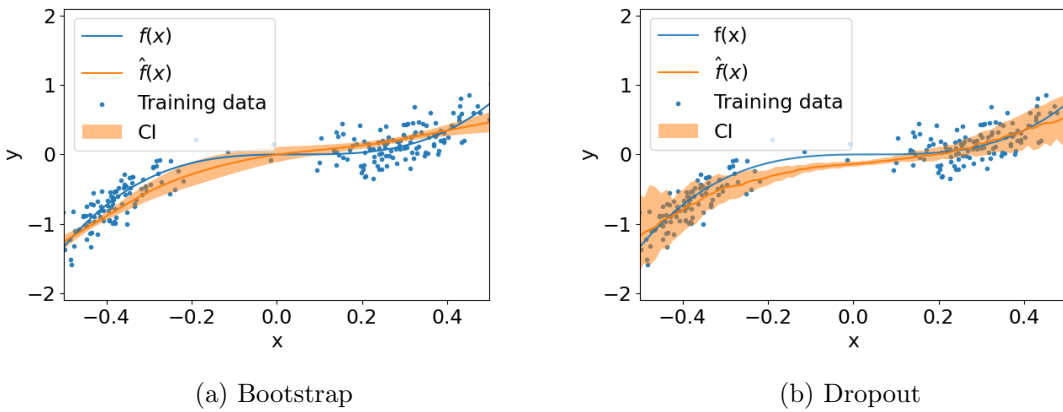


Figure 8: These two figures give 80% CIs using the naïve bootstrap (a) and Monte Carlo dropout (b). The blue line is the true function and blue dots give the training data. The same function and noise were used as when making Figure 4 with the difference that the covariates are not uniformly sampled. Even though the dropout approach gave a slightly better PICP score (0.831 versus 0.868), the CIs do not demonstrate better behaviour than those made with the bootstrap.

We simulated the data a total of 100 times to further demonstrate this behaviour. We can see in Figure 9(a) that in all 100 simulations both methods got a reasonable PICP score. If we look, however, at the CICF for x values between -0.2 and 0.1 we notice that dropout was not able to determine the uncertainty accurately. This information is only available if we use simulated data where the true function is known.

5.5 Boston Housing

So far we only used a simple one-dimensional simulation in our testing procedure. A good testing procedure should: 1 - be representative for real-world problems, and 2 - allow easy comparison between different methods. The data sets that are currently being used, listed in Table 1, meet these criteria. As we just demonstrated, however, it is desirable to simulate the data to get more insights in the accuracy of the uncertainty estimates. A solution would be to set up simulations based on data sets that are currently being used. In the following

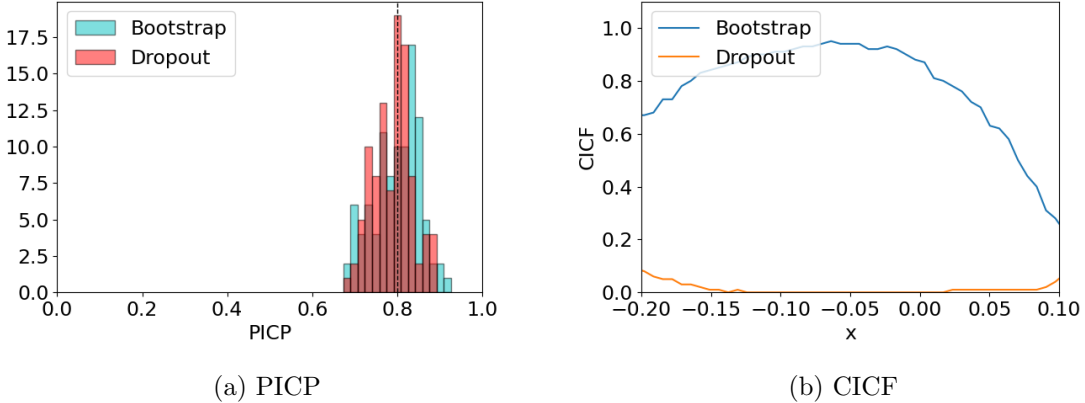


Figure 9: This figure demonstrates that a good PICP value (a) does not guarantee desirable behaviour of the epistemic uncertainty estimates. The region between -0.2 and 0.1 contained fewer data points. This figure, combined with Figure 8, demonstrates that both methods behave very differently in areas of limited data, something that is not detectable by merely evaluating the predictive uncertainty on a test set.

algorithm we give a suggestion how we could set up a simulation that resembles the Boston Housing data set.

Algorithm 3: Pseudo-code to simulate data based on the Boston Housing data set

- 1 Train a random forest on (X, Y) and use this predictor as the true function $f(\mathbf{x})$;
- 2 Calculate the residuals, $(Y - f(X))$;
- 3 Train a second random forest that predicts the residuals squared as a function of \mathbf{x} and use this predictor as the true variance $\sigma^2(\mathbf{x})$;
- 4 Simulate a new data set: $X_{\text{new}} = X$, $Y_{\text{new}} \sim \mathcal{N}(f(X), \sigma^2(X))$;
- 5 **Return:** $(X_{\text{new}}, Y_{\text{new}})$;

As an illustration we implemented this idea using two random forests with 100 trees, and max depth 3. We do not attempt to simulate new \mathbf{x} values as it would be difficult to get the dependencies between the covariates correct. We divided the generated data set in a train, test, and validation set of sizes 366, 100, and 40. The validation set is used by the bootstrap to determine the estimate of the aleatoric noise. The same bootstrap and dropout procedures as in the previous subsections were used to obtain PIs and CIs. In Figure 10(a) we can see that the PICP was a little too high, but quite close to the desired value of 0.8 in most of the simulations. In Figure 10(b) we can see, however, that for almost every \mathbf{x} the prediction intervals were either too large or too small. We see a similar trend if we look at the CICP in Figure 10(c). The bootstrap method consistently had a CICP that was too low, while the dropout method had a CICP that was too high. In Figure 10(d) we

can see that this was caused by a larger number of x values where the bootstrap method had a very low coverage fraction. This enforces the argument that simply looking at the performance on a single test set is far from optimal. It also shows that it is possible to apply this simulation-based testing procedure to representative data sets.

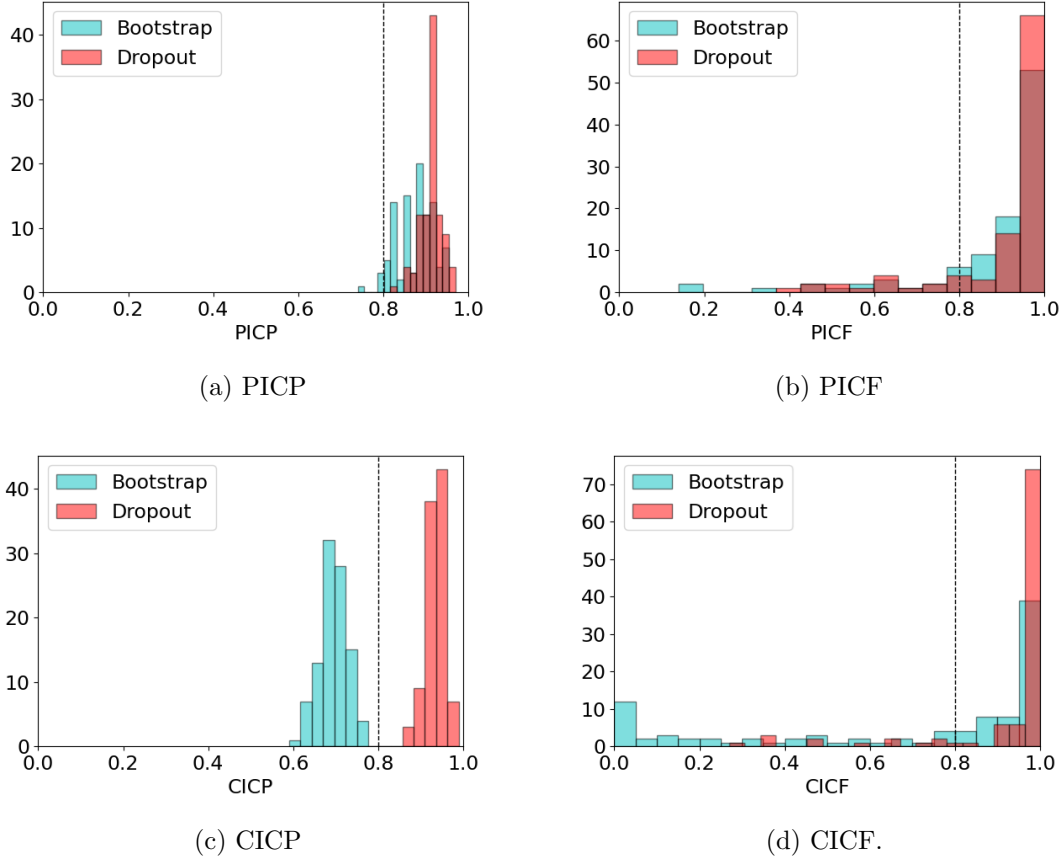


Figure 10: These histograms give the different PICP, PICF, CICP, and CICF values using the bootstrap and dropout approach on the Boston Housing simulation. The PICP and CICP values are obtained by calculating the coverage fraction of the PIs and CIs on the test set in each simulation. The PICF and CICF values are obtained by calculating the coverage fraction of the PIs and CIs for each test data point taken over all the simulations. In this simulation we constructed 80% PIs and CIs. For the PICF, bootstrap has a Brier score of 0.034 and average width of 0.796. Dropout has a Brier score of 0.029 and an average width of 0.979. For the CICF, bootstrap has a Brier score of 0.147 and average width of 0.378. Dropout has a Brier score of 0.042 and average width of 0.884. We once more observe that a good PICP value gives no guarantees for the actual performance of either the PI or CI on individual data points.

6. Conclusion

We conclude that the testing methodology applied to many recent publications for evaluating the quality of uncertainty estimates leaves a lot of room for improvement. These testing procedures rely on evaluating the predictive uncertainty, which is a combination of the aleatoric and epistemic uncertainty, on a previously unseen test set. The epistemic uncertainty is not independent over \boldsymbol{x} and it is therefore not optimal to assess the quality of its estimate in a single data set. We also showed that a good predictive uncertainty overall is not necessarily indicative of a good epistemic or aleatoric uncertainty estimate.

To overcome these problems, we propose simulation-based testing. This facilitates direct evaluation of the quality of the epistemic uncertainty estimate. An intuitive approach is to make PIs and CIs and test the coverage fractions, per \boldsymbol{x} , over a large number of simulations. Possible quantitative metrics of the PIs and CIs are the Brier score and the average width of the intervals. This approach does come of course with some downsides. The computational demands for running these tests are higher and there is a need to simulate the data. We propose to set up simulations based on the data sets listed in Table 1. It is also possible to set up a simulation based on a data set of particular interest. The additional computational demands only play a role during the testing of these uncertainty quantification methods and not in their usage in practice.

6.1 Future Research

In order to compare different uncertainty estimation methods, it is necessary to use the same simulations. It would therefore be useful to create a number of benchmark simulations that can be used to test uncertainty estimates. We propose to base these simulations on the data sets in Table 1. In Section 5.5 we gave a simple demonstration of such a simulation. In this paper we only considered normally distributed noise. Different distributions would allow us to explicitly see what happens if the customary assumption of normality does not hold. The methods in this paper are based on this assumption but a method like quantile regression, for instance, is not.

We saw in Section 5 that a method that performs better on a test set need not have better behaving uncertainty estimates. With new benchmarks, it would be worthwhile to re-evaluate currently available methods for estimating uncertainty.

References

Arsenii Ashukha, Alexander Lyzhov, Dmitry Molchanov, and Dmitry Vetrov. Pitfalls of in-domain uncertainty estimation and ensembling in deep learning. *arXiv preprint arXiv:2002.06470*, 2020.

Yarin Gal. *Uncertainty in deep learning*. PhD thesis, University of Cambridge, 2016.

Yarin Gal and Zoubin Ghahramani. Dropout as a Bayesian approximation: Representing model uncertainty in deep learning. In *International Conference on Machine Learning*, pages 1050–1059, 2016.

Alex Graves. Practical variational inference for neural networks. In *Advances in neural information processing systems*, pages 2348–2356. Citeseer, 2011.

José Miguel Hernández-Lobato and Ryan Adams. Probabilistic backpropagation for scalable learning of Bayesian neural networks. In *International Conference on Machine Learning*, pages 1861–1869, 2015.

Tom Heskes. Practical confidence and prediction intervals. In *Advances in Neural Information Processing Systems*, pages 176–182, 1997.

Kurt Hornik, Maxwell Stinchcombe, and Halbert White. Multilayer feedforward networks are universal approximators. *Neural networks*, 2(5):359–366, 1989.

Eyke Hüllermeier and Willem Waegeman. Aleatoric and epistemic uncertainty in machine learning: A tutorial introduction. *arXiv preprint arXiv:1910.09457*, 2019.

Abbas Khosravi, Saeid Nahavandi, Doug Creighton, and Amir F Atiya. Comprehensive review of neural network-based prediction intervals and new advances. *IEEE Transactions on neural networks*, 22(9):1341–1356, 2011.

Balaji Lakshminarayanan, Alexander Pritzel, and Charles Blundell. Simple and scalable predictive uncertainty estimation using deep ensembles. In *Advances in Neural Information Processing Systems*, pages 6402–6413, 2017.

Qiang Liu and Dilin Wang. Stein variational gradient descent: A general purpose Bayesian inference algorithm. In *Advances in Neural Information Processing Systems*, pages 2378–2386, 2016.

Zhou Lu, Hongming Pu, Feicheng Wang, Zhiqiang Hu, and Liwei Wang. The expressive power of neural networks: A view from the width. *Advances in Neural Information Processing Systems*, 30:6231–6239, 2017.

Tullio Mancini, Hector Calvo-Pardo, and Jose Olmo. Prediction intervals for deep neural networks. *arXiv preprint arXiv:2010.04044*, 2020.

Tim Pearce. *Uncertainty in Neural Networks; Bayesian Ensembles, Priors & Prediction Intervals*. PhD thesis, University of Cambridge, 2020.

Tim Pearce, Alexandra Brintrup, Mohamed Zaki, and Andy Neely. High-quality prediction intervals for deep learning: A distribution-free, ensembled approach. In *International Conference on Machine Learning*, pages 4075–4084, 2018.

Hugh Salimbeni and Marc Deisenroth. Doubly stochastic variational inference for deep gaussian processes. In *Advances in Neural Information Processing Systems*, pages 4588–4599, 2017.